Carbohydrate Polymers 302 (2023) 120438

Contents lists available at ScienceDirect

Carbohydrate Polymers

journal homepage: www.elsevier.com/locate/carbpol

Synthesis and characterization of thiazolium chitosan derivative with enhanced antimicrobial properties and its use as component of chitosan based films

C. Muñoz-Nuñez [a,b], R. Cuervo-Rodríguez [c], C. Echeverría [a,b], M. Fernández-García [a,b,*], A. Muñoz-Bonilla [a,b,*]

[a] Instituto de Ciencia y Tecnología de Polímeros (ICTP-CSIC), C/Juan de la Cierva 3, 28006 Madrid, Spain
[b] Interdisciplinary Platform for Sustainable Plastics towards a Circular Economy-Spanish National Research Council (SusPlast-CSIC), Madrid, Spain
[c] Facultad de Ciencias Químicas, Universidad Complutense de Madrid, Avenida Complutense s/n, Ciudad Universitaria, 28040 Madrid, Spain

ARTICLE INFO

Keywords:
Chitosan
Thiazolium
Antimicrobial
Chitosan films

ABSTRACT

In this work, chemical modification of chitosan using cationic thiazolium groups was investigated with the aim to improve water solubility and antimicrobial properties of chitosan. Enzymatic synthesis and ethyl-3-(3-dimethylaminopropyl) carbodiimide/N-hydroxysuccinimide (EDC/NHS) chemistry were employed to synthesize and attach to chitosan through the amine groups the molecule bearing thiazolium moieties, quaternized 4-(2-(4-methylthiazol-5-yl) ethoxy)-4-oxobutanoic acid (MTBAQ). On the basis of Fourier transform infrared spectroscopy (FTIR), elemental analysis and solid state nuclear magnetic resonance (ssNMR), around 95 % of the available amine groups of chitosan (of 25 % degree of acetylation) reacted. The resulting derivative was water soluble at physiological pH and exhibit excellent antimicrobial activity against *Listeria innocua*, *Staphylococcus epidermidis*, *Staphylococcus aureus* and Methicillin Resistant *S. aureus* Gram-positive bacteria (MIC = 8–32 μg/mL), whereas its efficiency decreases against fungi *Candida albicans* and *Eschericia coli* Gram-negative bacterium. Subsequently, the thiazolium chitosan derivative was employed as antimicrobial component (up to 7 wt%) of chitosan/glycerol based films. The incorporation of the chitosan derivative does not modify significantly the characteristics of the film in terms of thermal and mechanical properties, while enhances considerably the antimicrobial activity.

1. Introduction

Natural based polymers, such as polysaccharides, are currently desired materials for replacement of products derived from nonrenewable resources in many applications (Muñoz-Bonilla et al., 2019). Among all polysaccharides, the most abundant and used in material science and technology are cellulose, starch, chitin and chitosan. In addition to their abundance and renewable origin, these biopolymers are biocompatible and biodegradable, those features make them attractive for biomedical applications as well as for food and cosmetic industries (Casadidio et al., 2019; Jayakumar et al., 2011). These polysaccharides present also many hydroxyl groups subjected to chemical modification via esterification, etherification and oxidation, among others, that can be used to improve properties or provide new activities to meet the requirement of a target application. Chitosan, in addition to hydroxyl groups, has amino groups, which open new opportunities of chemical modifications, for instance methylation reaction, reductive amination, etc. (Bakshi et al., 2020). Precisely this amine group is the responsible of the antimicrobial character of chitosan (Ke et al., 2021). Chitosan becomes soluble in aqueous media and positive charged as a result of the protonation of these amino groups at pH values below 6.5 (Pillai et al., 2009). To improve and extend the antimicrobial character of chitosan to physiological pH, chitosan has been chemically derivatized by reaction of the mentioned hydroxyl and amino groups. Quaternization of the amino groups is probably the most used reaction, which involves the formation of permanently positive-charged quaternary ammonium moieties (Jung et al., 2019; Phuangkaew et al., 2022; Wu et al., 2016). These quaternized chitosan derivatives can have excellent antibacterial properties and their activity typically increases as the quaternization degree augments (Shagdarova et al., 2019). In this

* Corresponding authors at: Instituto de Ciencia y Tecnología de Polímeros (ICTP-CSIC), C/Juan de la Cierva 3, 28006 Madrid, Spain.
E-mail addresses: martafg@ictp.csic.es (M. Fernández-García), sbonilla@ictp.csic.es (A. Muñoz-Bonilla).

https://doi.org/10.1016/j.carbpol.2022.120438
Received 24 October 2022; Received in revised form 1 December 2022; Accepted 3 December 2022
Available online 9 December 2022

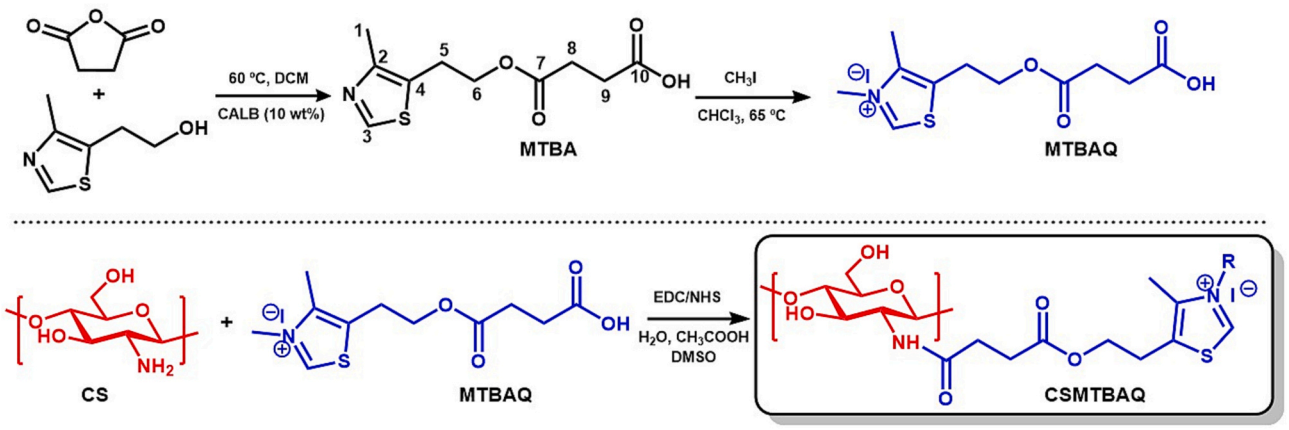

Fig. 1. Modification of chitosan by the incorporation of the cationic thiazolium molecule MTBAQ.

work, thiazolium moieties derived from the vitamin thiamine (B1) has been incorporated into chitosan to introduce permanent cationic charge. These thiazolium groups has been demonstrated to impart excellent antimicrobial activity to (meth)acrylic and itaconate polymers (Chiloeches et al., 2021; Tejero et al., 2015); however, to the best of our knowledge this thiazolium moiety has not been previously used in the preparation of chitosan derivatives. So, the incorporation of such group derived from vitamin B1 would allow the preparation of completely biobased chitosan polymer. To do this, efficient synthetic approaches, including enzymatic reaction and EDC/NHS coupling, have been employed with the intention to obtain high degree of substitution (Jung et al., 2019). The resulting chitosan derivative has been also used as antimicrobial component of blend films based on chitosan. Due to the outstanding film-forming properties, and decent mechanical and gas permeability properties of CS, based films have received particular attention as a bioabsorbable polymer in drug delivery films and in food packaging as, for instance, edible films. Indeed, the properties of such chitosan films can be improved by mixing with other components such as plasticizers, fillers or antimicrobial components (Policastro et al., 2022; Song et al., 2021; X. Zhang et al., 2021). Suitable approaches towards the improvement of their antimicrobial activity are the incorporation of metal and metal oxide nanoparticles, essential oils and organic compounds such as phenols, halogenated compounds and quaternary ammonium salts (Cadinoiu et al., 2022; Song et al., 2022; Zhang et al., 2022). However, the addition of such materials can present problems of aggregation or compatibility with the chitosan matrix and could drawback the properties of CS films in terms of biodegradability, mechanical properties or biocompatibility. In this work, the synthesized biobased chitosan derivative, with an expected well compatibility with chitosan matrix and similar properties, has been evaluated as antimicrobial agent in chitosan/glycerol films with potential applications in different fields.

2. Experimental part

2.1. Materials and reagents

Chitosan from shrimp shells (deacetylation degree > 75 %), succinic anhydride (≥99 %) and 5-(2-hydroxyethyl)-4-methylthiazole (98 %), iodomethane (MeI, 99.5 %), glycerol (Gly, 99 %), ethyl-3-(3-dimethylaminopropyl) carbodiimide (EDC, ≥98 %) and *N*-hydroxysuccinimide (NHS, 98 %) were purchased from Merck. Lipase B from *Candida antarctica* immobilized on microporous acrylic resin (CALB 5.000 U/g) was also obtained from Merck. All the organic solvents were of AR grade, dimethyl sulfoxide (DMSO), dichloromethane (DCM) and chloroform ($CHCl_3$) were provided by Scharlau. Deuterated chloroform ($CDCl_3$), water (D_2O), acetic acid (acetic acid-d_4) and dimethyl sulfoxide (DMSO-d_6) were acquired from Merck. Cellulose dialysis membranes (CelluSep T1) were purchased from Membrane Filtration Products, Inc.

For the antibacterial assay: sodium chloride solution (NaCl suitable for cell culture, BioXtra) and phosphate buffered saline powder (pH 7.4) were purchased from Merck. BBL Mueller–Hinton broth microbial growth medium was acquired from Becton, Dickinson and Company and the 96 well microplates from Thermo Fisher Scientific. Columbia agar (5 % sheep blood) plates were obtained from BioMérieux. American Type Culture Collection (ATCC): *Escherichia coli* (*E. coli*, ATCC 25922), *Listeria innocua* (*L. innocua* ATCC 33090), *Staphylococcus epidermidis* (*S. epidermidis*, ATCC 12228) and *Staphylococcus aureus* (*S. aureus*, ATCC 29213), *Staphylococcus aureus* resistant to methicillin and oxacillin (MRSA, ATCC 43300), *Candida albicans* (*C. albicans*, ATCC 200955) were used as bacterial strains, purchased from Thermo Scientific.

2.2. Synthesis of 4-(2-(4-methylthiazol-5-yl) ethoxy)-4-oxobutanoic acid (MTBA)

The acid MTBA was synthesized enzymatically using CALB enzyme (Fig. 1). A mixture of succinic anhydride (1.251 g, 12.5 mmol), 5-(2-hydroxyethyl)-4-methylthiazole (2.610 g, 18.2 mmol) and CALB (0.318 g, 10 wt% related to the reagents) was dissolved in 10 mL of DCM anhydrous and heated to 60 °C under stirring at 250 rpm during 10 h. Then, the flask was removed from the heating bath and cooled down. Enzyme beads were filtered off and cleaned thoroughly with DCM. The reaction mixture was then rotary evaporated to reduce the solvent volume. After concentration, the solution was precipitated in cold diethyl ether to afford MTBA (2.74 g, yield: 90 %) as white solid. The MTBA acid was characterized by ^{1}H NMR (see Fig. S1 of Supporting Information) and ^{13}C NMR (Fig. S2).

2.3. Quaternization of 4-(2-(4-methylthiazol-5-yl) ethoxy)-4-oxobutanoic acid (MTBAQ)

The thiazole groups of the previously synthesized MTBA were subjected to N-alkylation reaction with methyl iodide to provide quaternary ammonium groups (Fig. 1). MTBA (0.500 g, 2 mmol) was dissolved in 20 mL of chloroform and methylation reaction was carried out with five equivalents of methyl iodide (1.420 g, 10 mmol) per amine group at 65 °C (under reflux). Complete quaternatization was achieved after 72 h of reaction as confirmed by ^{1}H NMR (Fig. S3) and ^{13}C NMR (Fig. S4) spectroscopies of resultant acid MTBAQ. Solvent and methyl iodide excess were eliminated by rota-evaporation followed by dialysis and recovered by lyophilization (0.74 g, yield: 93 %).

2.4. Synthesis of N-alkyl chitosan derivative (CS-MTBAQ)

The MTBAQ carboxylic acid bearing cationic thiazolium groups was incorporated into chitosan through selective *N*-acylation of the amino group (Fig. 1). For this purpose, a coupling agent, EDC/NHS, was used to create a more active ester (Aryaei et al., 2014; Jung et al., 2019). Briefly, CS (0.500 g, 2.2 meq of amine groups) was dissolved in an aqueous solution of 2 wt% acetic acid in a round-bottom flask. Then, in another flask, MTBAQ (0.847 g, 2.2 mmol) and EDC (0.422 g, 2.2 mmol) were dissolved in 20 mL of DMSO and stirred for 20 min; subsequently, NHS (0.253 g, 2.2 mmol) was added and stirred for 10 min. This solution with the activated MTBAQ was dropwise added to the prior prepared chitosan solution and the reaction was conducted for 24 h at room temperature (Pranantyo et al., 2018). After the corresponding dialysis process against water for 3 days (MWCO 6–8 kDa) and subsequent lyophilization, the modified chitosan was obtained and characterized with several techniques (0.77 g, yield: 78 %).

2.5. Film preparation

Films based on chitosan and modified chitosan (CS-MTBAQ) were prepared by solution casting, using 30 wt% of glycerol as plasticizer (Dallan et al., 2007; Pavinatto et al., 2020). In brief, CS and CS-MTBAQ in mass ratio 90/10 was dissolved together with glycerol in 1 % acetic acid aqueous solution at a solid concentration of 1 % (*w/v*). Similarly, a solution of CS and glycerol in a 70:30 mass ratio (without modified chitosan) were also prepared for comparison purpose. Both solutions were poured into petri dishes, and left at room temperature to complete evaporation of the solvent to afford CS-film and CSMTBAQ-film.

2.6. Characterization

2.6.1. Nuclear magnetic resonance (NMR) spectroscopy

^{1}H and ^{13}C NMR spectra were recorded on a Bruker Avance III HD-400AVIII spectrometer at room temperature using as solvents DMSO-d_6. Solid state NMR was performed on an Avance TM 400WB Bruker instrument with a wide-mouth superconducting magnet (89 mm) operating at 9.4 T with a 400.14 MHz frequency.

2.6.2. Infrared spectroscopy

The infrared spectra of the prepared materials were obtained using a Perkin Elmer Spectrum Two instrument between 400 and 4000 cm^{-1} spectral range with a 4 cm^{-1} resolution and by compressing the samples (1 wt%) into KBr pellets. A background spectrum was acquired before every sample and all samples were vacuum-dried prior to measurement.

2.6.3. Elemental analysis

Elemental analysis was performed in a LECO CHNS-932 model PNT01 analyzer and the percentage of carbon, nitrogen, sulfur and hydrogen was quantified. On the basis of the estimated percentage the degrees of acetylation (DA) in chitosan and the degree of substitution (DS) in CSMTBAQ were calculated according to the following eqs. (J. Zhang et al., 2018):

$$C/N = \frac{(100 \times n_1 \times M_C) + (DA \times n_2 \times M_C)}{(100 \times n_3 \times M_N)} \quad (1)$$

$$C/N = \frac{(100 \times n_1 \times M_C) + (DA \times n_2 \times M_C) + (DS \times n_4 \times M_C)}{(100 \times n_3 \times M_N) + (DS \times n_5 \times M_N)} \quad (2)$$

where C/N is the mass ratio between carbon and nitrogen; M_C and M_N are the molar masses of carbon and nitrogen; n_1, n_2 and n_4 are the number of carbons of CS deacetylated, acetamido group and MTBAQ incorporated to the CS, respectively ($n_1 = 6$, $n_2 = 2$, $n_4 = 11$); n_3 and n_5 are the number of nitrogen of CS and MTBAQ added, respectively ($n_3 = 1$, $n_5 = 1$).

2.6.4. Thermal gravimetric analysis

Thermogravimetric analysis (TGA) of samples was performed on a TGA Q500 thermal analyzer (TA Instruments, US) at a heating rate of 10 °C/min from 25 to 800 °C, under air atmosphere (50 cm^3/min). The instrument was calibrated both for temperature and weight by standard methods.

2.6.5. Differential scanning calorimetry

Glass transition temperatures of the chitosan and modified chitosan were measured by differential scanning calorimeter. The experiments were performed on a TA Q2000 instrument (TA Instruments, US) under dry nitrogen (50 cm^3/min). The samples were equilibrated at 0 °C and heated to 400 °C at 10 °C/min. The temperature scale was calibrated from the melting point of high purity chemicals (lauric and stearic acid and indium). Samples were prepared in sealed aluminium pans and weight in an electronic autobalance.

2.6.6. Zeta potential measurements

The zeta potential measurements of CSMTBAQ were conducted at physiological pH values at 25 °C in a Zetasizer Nano series ZS (Malvern Instruments Ltd) using the Smoluchowski equation for electrophoretic mobility. The results are presented as the average of ten measurements.

2.6.7. X-ray diffraction

X-ray diffraction patterns of CS and CSMTBAQ were recorded at room temperature in the reflection mode using a Bruker D8 Advance diffractometer provided with a PSD Vantec detector (from Bruker, Madison, Wisconsin). CuK_α radiation ($\lambda = 0.15418$ nm) was used, operating at 40 kV. Samples were mounted on an appropriate holder and scanned between 2° and 60° (2θ) with a scanning step of 0.02°, and a collection time of 10 s per step.

2.6.8. Mechanical properties

Mechanical properties of the CS-film and CSMTBAQ-film were studied by tensile test measurements performed at room temperature on a DX2000 QTest Elite MTS dynamometer (MTS Systems, Eden Prairie, MN, USA), working at a stretching rate of 10 mm/min. Dog-bone specimens with gauge dimension of 20 mm in length and 2 mm in width, and a thickness of around 0.1 mm. At least five specimens were tested for each material.

2.7. Antimicrobial assays

The antimicrobial activity of the modified chitosan CSMTBAQ was evaluated by determining its minimum inhibitory concentration (MIC) against the bacterial strains L. *innocua*, *S. aureus*, *S. epidermidis*, *MRSA, C. albicans,* and *E. coli*, following a standard broth dilution method according to the Clinical Laboratory Standards Institute (CLSI) (CLSI, n.d., *Methods for Dilution Antimicrobial Susceptibility Tests for Bacteria That Grow Aerobically, Approved Standard-Ninth Edition, CLSI Document M07-A9, Clinical and Laboratory Standards Institute, Wayne, PA, 2012*). Bacterial and fungal strains were grown on 5 % sheep blood Columbia agar plates for 24 h and 48 h, respectively, at 37 °C. Then, microbial suspensions were prepared with saline solution to 10^8 colony-forming units (CFU)/mL (turbidity equivalent to ca. 0.5 McFarland turbidity standard). Subsequently, the suspensions were further diluted to 10^6 CFU/mL with fresh Mueller-Hinton broth. In parallel, a stock polymer solution of CSMTBAQ at a concentration of 2 mg/mL in Mueller-Hinton broth was prepared. As a general procedure, 100 μL of this polymer stock solution was placed in the first column of a 96-well round bottom microplate, 50 μL of broth was added into the rest of the wells, and 1:2 serial dilutions were made across the plate. Next, 50 μL of the microbial suspension was added in all the wells to yield a total volume of 100 μL and a microbial concentration of 5×10^5 CFU/mL. A positive control without polymer and a negative control without bacteria were also performed. The plates were incubated at 37 °C for 24 h or 48 h, for

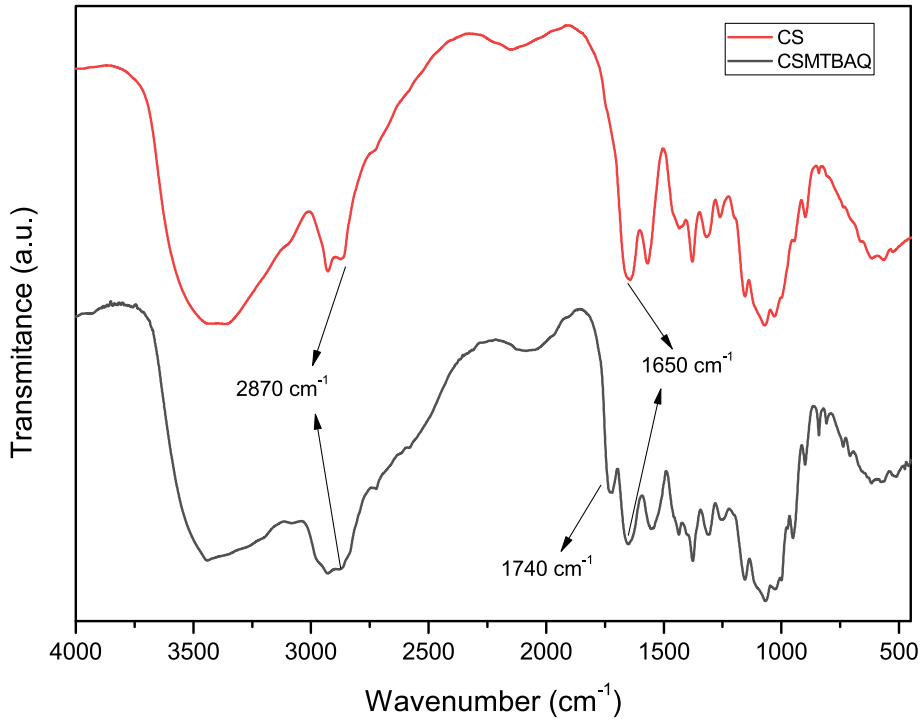

Fig. 2. FTIR spectra of CS and CSMTBAQ derivative.

bacteria and fungi respectively, and the MIC values were visually determined by checking the absence of bacterial growth.

The antimicrobial activities of the CS-film and CSMTBAQ-film were determined against the same microbial strains, following the E2149-20 standard method from the American Society for Testing and Materials (ASTM) (ASTM E2149-20, n.d., *Standard Test Method for Determining the Antimicrobial Activity of Antimicrobial Agents Under Dynamic Contact Conditions; ASTM International, Www.Astm.Org.*). Each film was placed in a sterile falcon tube with 9 mL of PBS. Then, 1 mL of the microbial suspension previously prepared in PBS ($\sim 10^6$ CFU/mL) were added (Cuervo-Rodríguez et al., 2017). Control experiments were also performed in the absence of sample. The tubes were shaken at 100 rpm during 24 h. After that, the microbial colonies were counted by the plate counting method after 24 h or 48 h incubation at 37 °C for bacteria and fungi, respectively. The reduction percentage was calculated in comparison to the control. The measurements were made at least in triplicate.

2.8. Statistical analysis

All experiments were performed at least in triplicates. One way analysis of variance (one-way ANOVA) followed by post-hoc Turkey's test was performed to determine significant differences at $P \leq 0.05$ among different groups for antimicrobial and mechanical properties.

3. Results and discussion

3.1. Synthesis and characterization of chitosan derivative CSMTBAQ

Initially, the 4-(2-(4-methylthiazol-5-yl) ethoxy)-4-oxobutanoic acid (MTBA) was successfully synthesized in high yield via enzymatic synthesis using CALB. The chemical structure of the MTBA was confirmed by ^{1}H NMR and ^{13}C NMR spectroscopy (Figs. S1 and S2 of Supporting Information). Subsequently, from the synthesized MTBA, quaternary thiazolium salt was prepared by reaction of MTBA with methyl iodide. The success of the *N*-alkylation reaction was demonstrated by ^{1}H NMR and ^{13}C NMR (see Figs. S3 and S4). In ^{1}H NMR spectrum, it can be clearly observed that the signal corresponding to the aromatic proton of 1,3-thiazole, —N═CH—S, at ~8.89 ppm shifted to ~10.05 ppm (C3—H) after the *N*-alkylation to obtain 1,3-thiazolium group, N+═CH—S. Likewise, in ^{13}C NMR spectrum, new signal at 41.0 ppm corresponding to the —CH_3 attached to the nitrogen of the thiazolium group (C11) is appreciated.

Once the quaternary ammonium molecule containing carboxylic acid functionality, MTBAQ, was synthesized, next step was its incorporation to the amine groups of chitosan via EDC/NHS chemistry as shown in Fig. 1.

The obtained chitosan derivative (CSMTBAQ) with quaternary ammonium salt linked through an amide group and with potential antimicrobial activity was extensively characterized by common techniques. FTIR spectra of raw (CS) and modified chitosan (CSMTBAQ) are shown in Fig. 2. The spectrum of CS exhibits the characteristic bands of this biopolymer as reported in literature (Brugnerotto et al., 2001; Lawrie et al., 2007), a broad band centered at 3450 cm^{-1} attributed to hydroxyl groups, the N—H stretching vibration at 3360 cm^{-1}, alkyl C—H stretching bands between 3000 and 2800 cm^{-1}, stretching vibration band of the carbonyl in the amide at 1650 cm^{-1}, and N—H bending at 1560 cm^{-1}. In addition to these bands proceeding from CS, new bands appeared in the spectrum of CSMTBAQ, which confirms the incorporation of the thiazolium containing molecules into CS. Mainly, a new band appears at 1740 cm^{-1} that can be associated to the —C═O stretching band of the ester group presented in MTBAQ. The region between 3035 and 2760 cm^{-1} associated with the C—H and═C—H stretching vibration modes also exhibits noticeable changes, with bands above 3000 cm^{-1} ascribed to aromatic bonds (Piegat et al., 2019).

From FTIR spectra of CS and CSMTBAQ the degree of acetylation (DA) and degree of substitution (DS) can be estimated. Before calculating DS in CSMTBAQ, the DA of the raw CS was experimentally determined through a correlation between the intensity of the amide band (1650 cm^{-1}) to the C—H stretching band (2870 cm^{-1}) (Baxter et al., 1992; Kasaai, 2008), following the next equation:

$$\frac{A_{1650}}{A_{2870}} = 0.0132 \times DA + 0,0012 \quad (3)$$

Table 1
Degree of acetylation (DA) and degree of substitution (DS) calculated based on the relationship between the absorbance value at 1650 cm^{-1} (A_{1650}) and at 2870 cm^{-1} (A_{2850}).

Sample	A_{1650}	A_{2870}	A_{1650}/A_{2870}	DA (%)	DS (%)
CS	70.6	70.4	1	26	–
CSMTBAQ	72.2	57.1	1.3	26	69

Table 2
Percentage of carbon, hydrogen and nitrogen, and degree of acetylation (DA) and degree of substitution (DS) calculated by elemental analysis.

Sample	%C	%H	%N	%S	C/N	DA (%)	DS (%)
CS	40.6 ± 0.3	6.7 ± 0.3	7.2 ± 0.3	–	5.6	28	–
CSMTBAQ	33.1 ± 0.3	5.9 ± 0.3	4.8 ± 0.3	5.2 ± 0.3	6.9	28	67

The calculated DA value of raw CS was found to be 26 %, very near the value gave by the company (25 %). Taking into account that CS was not previously deacetylated, DS was calculated referred to the modification of the part that is not acetylated (maximum 74 %). The DA in CSMTBAQ calculated by Eq. (3) was found to be 96 %, corresponding to a DS of about 70 % (see Table 1).

Similarly, the DA and DS for CS and CSMTBAQ, respectively, were calculated on the basis of the percentages of carbon and nitrogen estimated by elemental analysis according to the Eqs. (1) and (2). The results are collected in Table 2. Again, the DA of raw CS calculated by elemental analysis is very close to the value obtained from the commercial specifications and the DS in the CSMTBAQ derivative was found to be 67 %, very similar to that found by FTIR analysis. The presence of sulfur in the CSMTBAQ sample also confirms the incorporation of the thiazolium molecules into chitosan.

The modification of chitosan with thiazolium groups was also corroborated by solid state ^{13}C NMR. In the spectra showed in Fig. 3, it is clear the presence of new signals in chitosan derivative CSMTBAQ, in addition to chitosan signals. On one hand, ^{13}C NMR of CS shows the signals at 174.13 (C═O), 104.99 (C1), 83.52 (C4), 75.27 (C5, C3), 61.28 (C6), 57.70 (C2) and 23.76 ppm (CH_3) (Ottey, 1996; Taboada et al., 2004). Whereas, in the CSMTBAQ spectrum, it is also principally observed a new signal at 99.93 ppm associated to —C—O—CO— of the MTBAQ molecule and the signal at 41.0 ppm related to the $\underline{C}H_3$-N^+. The greater intensity of the signal assigned to the —C═O and —CH_3 at 104.99 and 24.39 ppm, respectively, is also an evidence of derivative formation. From the NMR spectra it is also possible to determine the DA and DS from the relative intensity of the signals according to the equations below (Van de velde & Kiekens, 2004):

$$DA = \frac{I_{CH_3}}{(I_{C1} + I_{C2} + I_{C3} + I_{C4} + I_{C5} + I_{C6})/6} \quad (4)$$

$$DS = \frac{I_{C_{14}}}{(I_{C_1 - C_{13}} + I_{C_{15}} + I_{C_{16}})/16} - DA \quad (5)$$

The DA value of CS and the DS value of CSMTBAQ were calculated as 25 % and 63 %, respectively, values very similar to results estimated before by FTIR and elemental analysis.

Next, the crystalline properties of raw chitosan and chitosan derivative were presented by XRD patterns in Fig. 4.

Chitosan in the solid state is organized in crystalline regions that coexist with amorphous regions, so the structure of the biopolymer has high stability (Morsy et al., 2019). The raw chitosan shows the characteristic main peaks at 2θ of 9.4° and 20.0°, corresponding to crystalline reflections (020) and (110), assigned to crystal form one and crystal form two, respectively. This fact was an indication of high degree of crystallinity of chitosan. Compared to chitosan, the chitosan derivative CSMTBAQ exhibits a dramatic decrease of crystallinity due to the disruption of the inter- and extra-molecular hydrogen bonding and therefore, of the ordered structure of the chitosan (Pandit et al., 2020).

Next, the thermal properties of the CSMTBAQ derivative were studied and compared to the raw chitosan. The thermal stability was analyzed by TGA, as represented in Fig. 5.

Two main steps of degradations were observed in both samples, CS and CSMTBAQ. The first mass loss process at temperatures below 100 °C, was assigned to the loss of water bounded to the chitosan chemical structures mainly by hydroxyl and amine groups and also through the new functional groups incorporated in the CSMTBAQ derivative (Zakaria et al., 2012). The second stage observed in CS, was the primary degradation, which starts at 247 °C and proceeds at a maximum rate temperature of 275 °C. This process involves the elimination of

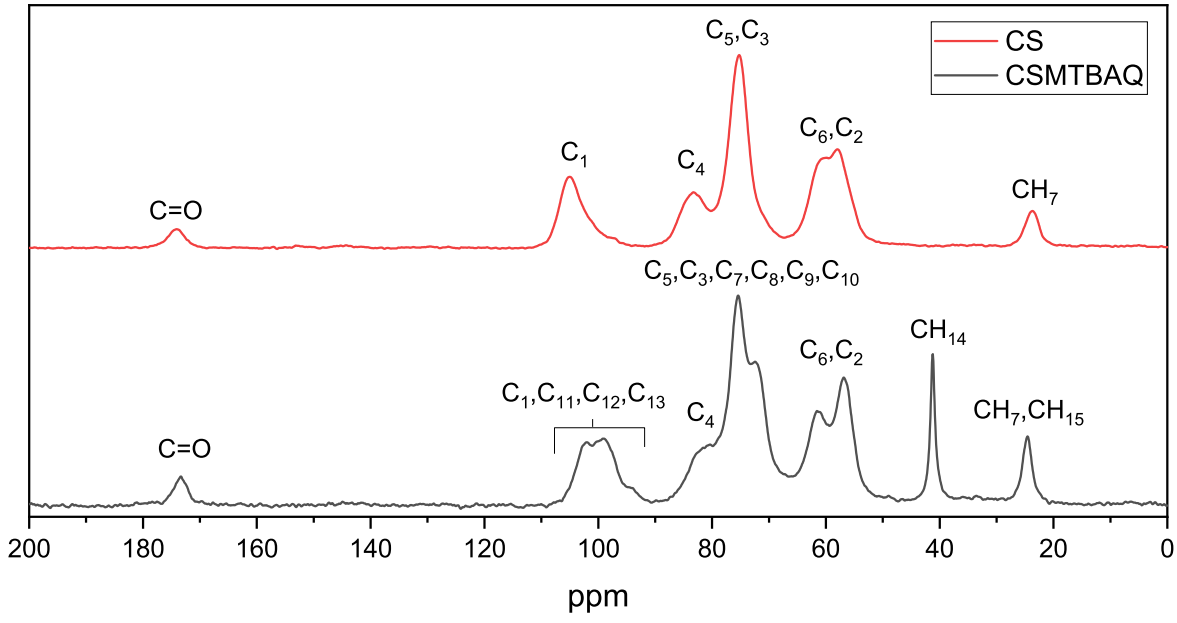

Fig. 3. Solid state ^{13}C NMR of CS and CSMTBAQ.

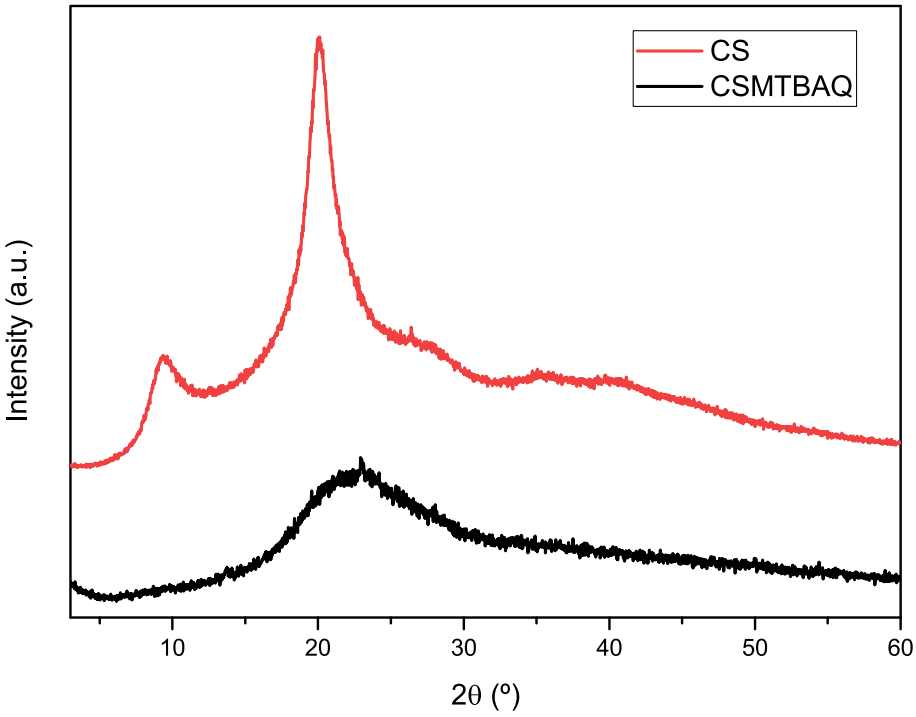

Fig. 4. X-ray diffraction patterns of CS and CSMTBAQ.

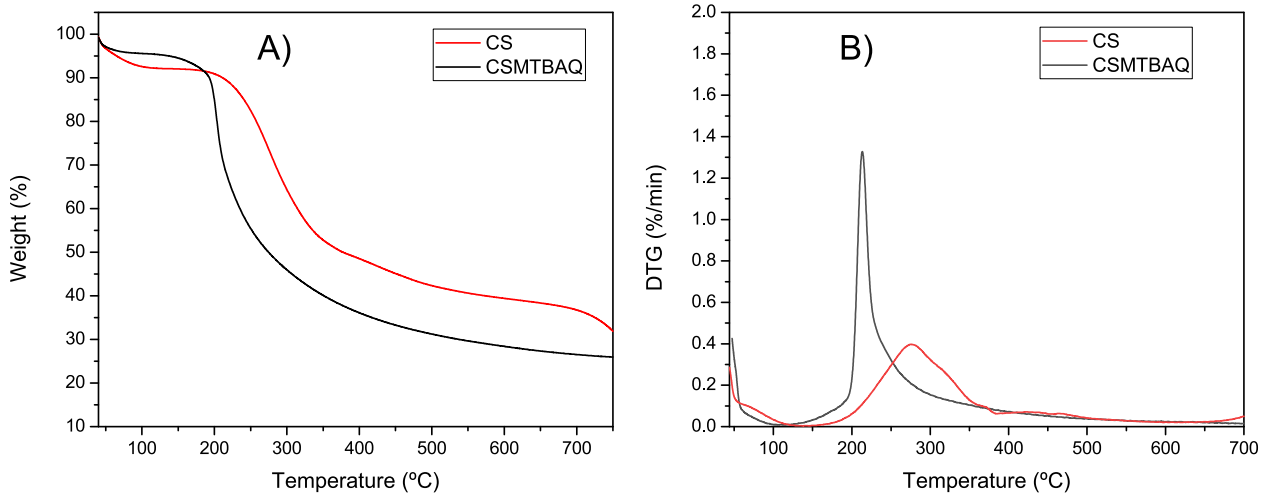

Fig. 5. A) Thermogravimetric curves and B) their derivative (DTG) of CS and CSMTBAQ.

volatile compounds, low-molecular-weight molecules, and functional groups. A large residue was appreciated as normally reported before, due to the crosslinking of chitosan during thermal decomposition (Moussout et al., 2016). The second decomposition stage for the CSMTBAQ clearly occurs at lower temperature, with a temperature at maximum weight-loss rate of 213 °C. The results demonstrate the loss of thermal stability for the modified CSMTBAQ compared to the CS (Yeh et al., 2006). The crystalline degree decreases with the incorporation of the MTBAQ moieties and therefore, the thermal stability is compromised.

The thermal behavior of the chitosan derivative was also studied by DSC and compared to neat CS and is displayed in Fig. 6.

The DSC curve of raw chitosan showed a broad endothermic peak around 100 °C, which is associated to water evaporation and an exothermic peak around 300 °C, related to the decomposition process of chitosan including decomposition of amines (Guinesi & Cavalheiro, 2006; Kasaai, 2009). In fact, the exothermic effect might result from crosslinking reactions following the destruction of amino groups occurring during thermal degradation (Wanjun et al., 2005). This exothermic peak takes place at temperature similar to the decomposition temperature determined by TGA. In the case of CSMTBAQ derivative, a broad endothermic peak associated to evaporation of bound water was also appreciated. However, the position and enthalpy of the peak is different, indicating its different water holding capacity and interaction strength(Bashir et al., 2019; Harish Prashanth, 2002). Regarding the second thermal event recorded, there is a clear difference between the two thermograms. Whereas in raw CS an exothermic peak was observed, in the CSMTBAQ a sharp endothermic peak was clearly appreciated. The endothermic peak of CSMTBAQ appears at much lower temperature, around 210 °C, than the peak associated to the decomposition of raw CS. This peak corresponds to a decomposition of highly substituted chitosan with low content of primary amine groups, and also

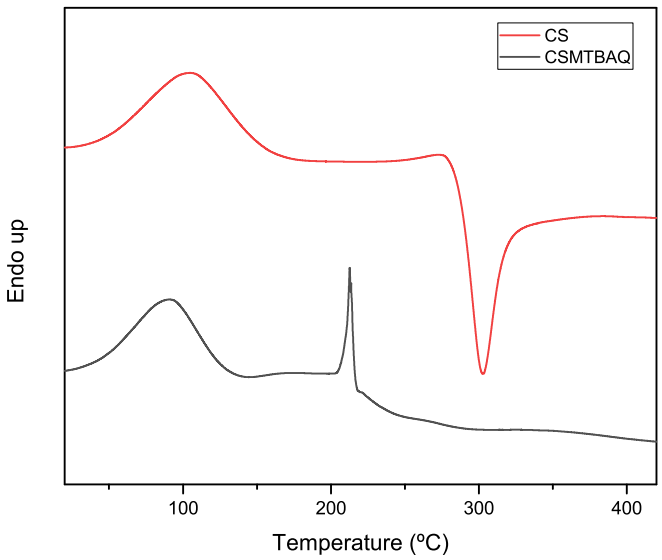

Fig. 6. DSC curves of CS and CSMTBAQ.

corroborates the thermal stability decrease as a result of the chemical modification (Wanjun et al., 2005).

3.2. Antimicrobial activity of chitosan derivative CSMTBAQ

The successful incorporation of the thiazolium groups with potential antimicrobial activity was confirmed by different techniques. The main advantages of this chitosan derivative are its improved water solubility and its polycationic feature at physiological pH. The chitosan has a pKa of 6.5 and becomes polycation only under acidic conditions (Ahmed et al., 2021; Chang et al., 2015; Ding et al., 2019). Then, at physiological pH, the chitosan forms aggregates due to loss of charge and turns insoluble in water. In the case of CSMTBAQ derivative, the introduction of the cationic thiazolium groups increases considerably the aqueous solubility at neutral pH environments as the polymer presents positive charge density, with zeta potential value of 27.6 ± 7.0 mV (Phuangkaew et al., 2022). Then, it is also expected an improved antimicrobial efficiency. The broth microdilution method was used to determine the MIC values of chitosan derivative against a variety of microbial strains, whereas neat chitosan was not soluble in broth medium and their MIC values could not be estimated. Table 3 collects MIC values of CSMTBAQ estimated against all tested microorganisms including L. *innocua*, *C. albicans*, *S. epidermidis*, *S. aureus*, *E. coli* and a clinically significant resistant bacterium, MRSA.

A significant antimicrobial activity against Gram-positive bacteria was appreciated, with MIC values as low as 8 μg/mL for *L. innocua* and *S. epidermidis* and 31 μg/mL for *S. aureus* and MRSA. However, this chitosan derivative shows moderate activity against the fungi *C. albicans* and was not active against *E. coli* Gram-negative bacteria. Typically, unmodified chitosan exhibits poor activity against both Gram-positive and Gram-negative bacteria with the MIC values higher than 256 μg/mL (Cele et al., 2020), and this chitosan derivative bearing a thiazolium groups demonstrated a significant improvement activity on Gram-positive bacteria with MIC ranging from 8 to 31 μg/mL, values lower or comparable with other chitosan derivatives reported in literature (Cele et al., 2020; Si et al., 2021). But, it was ineffective against Gram-negative strain. This low activity against Gram-negative *E. coli* bacteria can be ascribed to the lack of hydrophobic groups. Hydrophobicity is also a key factor affecting the antimicrobial activity as enhanced its ability to permeabilize the cell wall (Sahariah & Másson, 2017).

3.3. Antimicrobial films based on CS and CSMTBAQ

Chitosan is an attractive biopolymer for food packaging due to its biodegradability, moderate antimicrobial properties as well as its film forming property. Chitosan based films or coatings have extensively used in food industry to extend shelf-life of fresh products, such as meat, bread, and cheese (Kumar et al., 2020). However, as commented before, its antimicrobial properties are limited. Then, incorporation of antimicrobial agents or particles into the films has been proposed as attractive approach to improve such antimicrobial properties since blending is one of the most effective and efficient process of film formation for large-scale manufacturing. In this work, the synthesized CSMTBAQ derivative was employed as minor component of blend film based on neat chitosan as matrix or main component, and glycerol as plasticizer. Cast films were prepared with 30 wt% glycerol, 63 wt% CS and 7 wt% CSMTBAQ (CS/CSMTBAQ-film). The obtained film was characterized by different techniques and compared with a CS based film (CS-film), including the study of its mechanical and antimicrobial properties.

Fig. 7 shows the FTIR spectra of both films, in which are observed mainly the key characteristics bands of chitosan.

In the CS/CSMTBAQ-film blend, the band at 1740 cm^{-1} from the carbonyl group of the MTBAQ moiety is appreciated with very low intensity due to the low amount of CSMTBAQ incorporated into the blend film. Also, the band at 2870 cm^{-1} increases in intensity as a result of the CSMTBAQ derivative. Glycerol also provokes small changes in the spectrum, as interacts with CS through hydrogen bonds, i.e., the bands between 1330 and 1420 cm^{-1} corresponding to the bending in plane of OH and —CH_2— of the carbohydrate ring (Al-Masry et al., 2021).

The films were characterized by XRD as represented in Fig. 8. Both films presented very similar patterns with the two main peaks of chitosan at 2θ 9.4° and 20.1°. However, the peaks intensities in the film

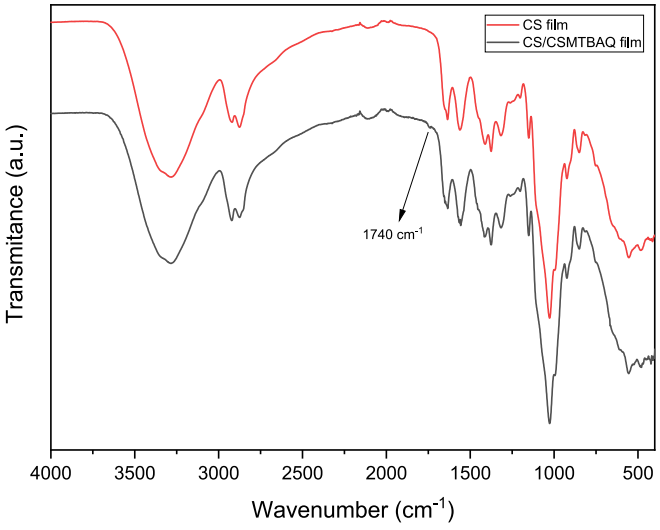

Fig. 7. FTIR spectra of CS-film and CS/CSMTBAQ-film.

Table 3
Antibacterial activities of the resulting CSMTBAQ.

MIC (μg/mL)						
	L. innocua	*S. epidermidis*	*S. aureus*	MRSA	*C. albicans*	*E. coli*
CSMTBAQ	8	8	31	31	250	>1000

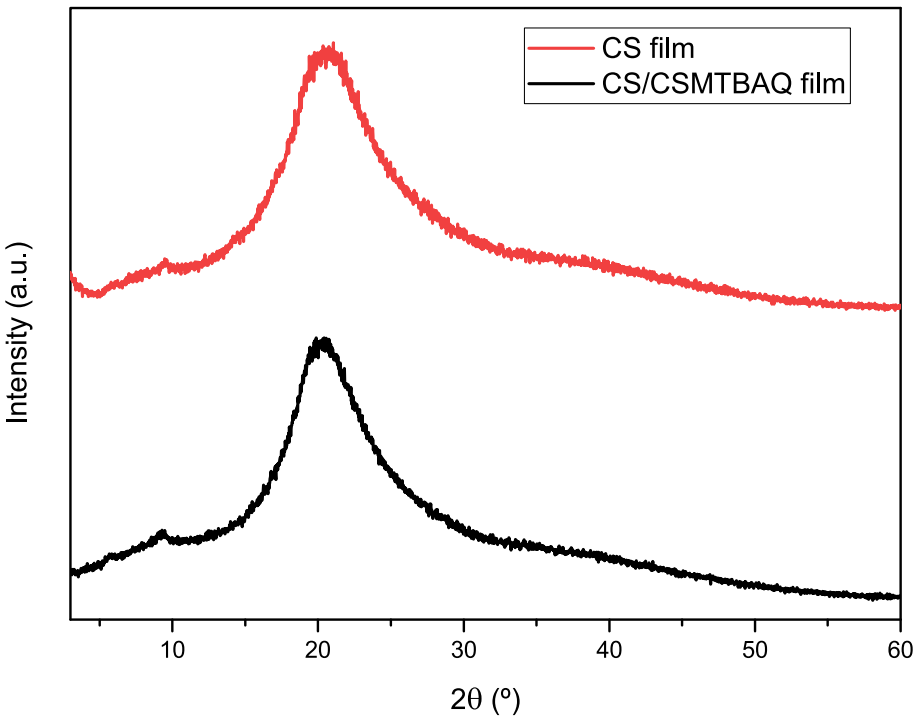

Fig. 8. XRD patterns of CS-film and CS/CSMTBAQ-film.

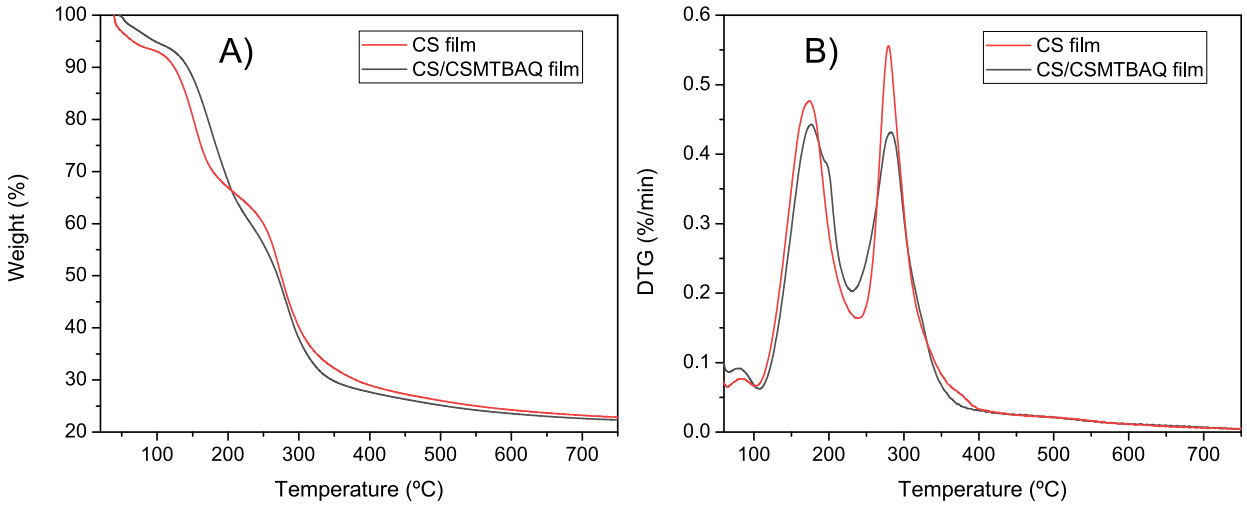

Fig. 9. A) Thermogravimetric curves and B) their derivatives of CS-film and CS/CSMTBAQ-film.

decrease with respect to the initial chitosan, as is displayed in Fig. 6, due to the loss of crystallinity associated to the content of glycerol and to the film formation process (Jayasuriya et al., 2013).

The thermal stability of the films was then studied by the TGA. Fig. 9 shows thermograms of CS-film and CS/CSMTBAQ-film, both containing 30 wt% of glycerol. In both samples, a first weight loss was observed due to water evaporation. The weight change in the second stage from 110 °C to 240 °C resulted from glycerol decomposition (Wang et al., 2019), with a mass loss very close to the weight percentage of glycerol added to the films. Also, a shoulder at around 200 °C was observed in the DGT curve of CS/CSMTBAQ films that can be associated to the CSMTBAQ derivative incorporated at 7 wt%. Subsequently, the main decomposition region of chitosan (240–400 °C) was visible in both films with a temperature of maximum degradation rate at 278–280 °C (Ma et al., 2019).

The effect of the incorporation of CSMTBAQ derivative in chitosan/glycerol film was also analyzed by DSC. Similarly to other techniques, slightly modifications were only observed in DSC thermograms as shown in Fig. 10. The first endothermic peak attributable to the energy required to vaporize water occurred at different temperature range (Maria et al., 2016). A shift to lower temperature was clearly appreciated in the film containing CSMTBAQ, suggesting that the interactions with water molecules were rather weaker in comparison with the CS-film sample. Similar results were previously found for CS and CSMTBAQ derivative (see Fig. 6), which can be due to the reduction of amine groups of chitosan as a consequence of the substitution reaction and formation of the amide group in CSMTBAQ derivative. Then, the second endothermic peak at around 240 °C corresponds to glycerol (Kaya et al., 2018; Liang et al., 2009). Finally an exothermic broad peak was observed in both films associated to the thermal degradation of chitosan, which is a bit broader in CS/CSMTBAQ-film due to the presence of the CSMTBAQ derivative.

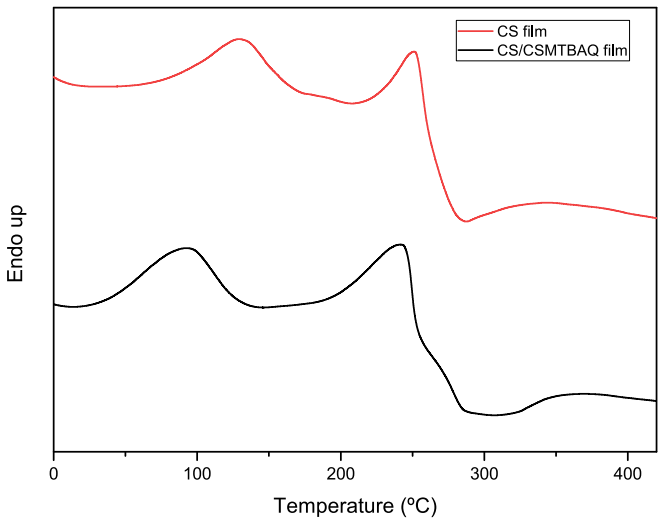

Fig. 10. DSC thermograms of CS-film and CS/CSMTBAQ-film.

Table 4
Mechanical properties of CS-Film and CS/CSMTBAQ-Film, elongation at break (%E), elastic modulus (E) and the maximal tensile strength (TS).

Sample	*E (MPa)*	*TS (MPa)*	*ε (%)*
CS-film	41.2 ± 7.1[a]	21.5 ± 3.4[a]	40.6 ± 3.3[a]
CS/CSMTBAQ-film	47.6 ± 4.5[a]	24.7 ± 4.7[a]	40.0 ± 3.7[a]

Values having the same letter are not significant different for Tukey test (Significance level of $P \leq 0.05$).

The mechanical properties of the chitosan based films were investigated as a function of the incorporation of CSMTBAQ derivative in the chitosan/glycerol film. Table 4 summarizes the elongation at break (ε), elastic modulus (E) and the maximal tensile strength (TS) values obtained for CS-film and CS/CSMTBAQ-film. As can be seen, elongation at break was high in both films in comparison with neat chitosan films reported in literature due to the content of glycerol plasticizer included in the formulation, which improves the mobility of chitosan chains by reducing intermolecular attraction (Nouri et al., 2018; Sabbah et al., 2019; Ziani et al., 2008). As expected, the tensile strength and elastic modulus are much lower than that reported in literature for chitosan films as the flexibility of the films increases considerable with the addition of glycerol. When CS-film and CS/CSMTBAQ are compared, no significant differences were appreciated on mechanical properties, meaning that the incorporation of 7 wt% of the antimicrobial derivative did not considerably affect the mechanical performance.

Next, the antimicrobial activity of chitosan films containing low content of CSMTBAQ derivative was evaluated against a variety of microbial strains; including Gram-positive and Gram-negative bacteria, resistant bacteria and fungi (Fig. S5 of Supporting Information displayed pictures of the agar plates used for microbial counting to determine microbial reduction percentage). The results are presented in Fig. 11. It is observed that the CS-film exhibits reasonable antimicrobial activity against the tested microorganisms, due to its cationic character. In addition, the incorporation of the CSMTBAQ improves the antibacterial performance of the film on most of the strains, with the exception of *E. coli*, which was expected taking into consideration the high MIC value obtained against this Gram-negative strain.

4. Conclusions

Chitosan was successfully modified through its amine groups using a

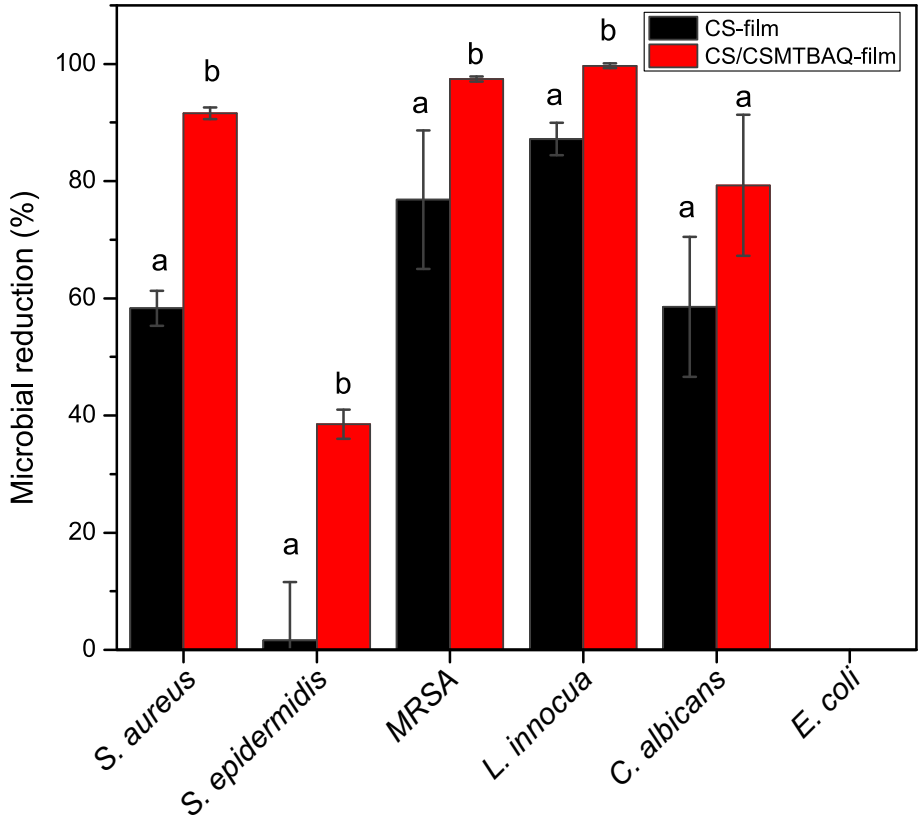

Fig. 11. Antimicrobial activity of CS-film and CS/CSMTBAQ-film estimated as microbial reduction percentage. Data were compared using one-way analysis of variance (ANOVA) followed by Tukey's test. Bars with different superscripts are significantly different at $P \leq 0.05$.

thiazolium derivative of vitamin B1 (MTBAQ) with antimicrobial properties. Efficient reaction including enzymatic reaction and EDC/NHS coupling chemistry was employed to obtained high degree of substitution of around 96–98 %. The resulting chitosan derivative was water soluble at physiological pH, presented permanent positive charge with a zeta potential value of 27.6 ± 7.0, and was found very active against Gram-positive bacteria including methicillin-resistant *Staphylococcus aureus*. The use of this derivative CSMTBAQ as minor component of chitosan/glycerol blend films was also demonstrated. The incorporation of only 7 wt% of CSMTBAQ improves the antimicrobial performance of the films while film forming properties as well as the mechanical and thermal behavior are almost maintained. Therefore, this derivative with thiazolium groups could have the potential to be applied as an antimicrobial agent in uses such as food packaging.

CRediT authorship contribution statement

C. Muñoz-Nuñez: Investigation, Methodology. **R. Cuervo-Rodríguez:** Methodology. **C. Echeverría:** Methodology, Formal analysis. **M. Fernández-García:** Supervision, Writing – review & editing. **A. Muñoz-Bonilla:** Supervision, Writing – review & editing.

Declaration of competing interest

The authors declare that they have no known competing financial interests or personal relationships that could have appeared to influence the work reported in this paper.

Data availability

Data will be made available on request.

Acknowledgments

This work was funded by the MICINN (PID2019-104600RB-I00), the Agencia Estatal de Investigación (AEI, Spain) and Fondo Europeo de Desarrollo Regional (FEDER, EU). C. Muñoz-Nuñez also acknowledges MICINN for her FPI fellowship PRE2020-093596. Authors thanks V. Hevilla for his help with enzymatic synthesis.

Appendix A. Supplementary data

Supplementary data to this article can be found online at https://doi.org/10.1016/j.carbpol.2022.120438.

References

Ahmed, R., Hira, N.u.a., Fu, Z., Wang, M., Halepoto, A., Khanal, S., … Guo, X. (2021). Control and preparation of quaternized chitosan and carboxymethyl chitosan nanoscale polyelectrolyte complexes based on reactive flash nanoprecipitation. *ACS Omega, 6*(38), 24526–24534. https://doi.org/10.1021/acsomega.1c02185

Al-Masry, W. A., Haider, S., Mahmood, A., Khan, M., Adil, S. F., & Siddiqui, M. R. H. (2021). Evaluation of the thermal and morphological properties of γ-irradiated chitosan-glycerol-based polymeric films. *Processes, 9*(10), 1783. https://doi.org/10.3390/pr9101783

Aryaei, A., Jayatissa, A. H., & Jayasuriya, A. C. (2014). Mechanical and biological properties of chitosan/carbon nanotube nanocomposite films. *Journal of Biomedical Materials Research Part A, 102*(8), 2704–2712. https://doi.org/10.1002/jbm.a.34942

ASTM E2149-20, n.d.ASTM E2149-20, Standard Test Method for Determining the Antimicrobial Activity of Antimicrobial Agents Under Dynamic Contact Conditions; ASTM International, www.astm.org. (n.d.).

Bakshi, P. S., Selvakumar, D., Kadirvelu, K., & Kumar, N. S. (2020). Chitosan as an environment friendly biomaterial – a review on recent modifications and applications. *International Journal of Biological Macromolecules, 150*, 1072–1083. https://doi.org/10.1016/j.ijbiomac.2019.10.113

Bashir, S., Teo, Y. Y., Ramesh, S., Ramesh, K., Rizwan, M., & Rizwan, M. (2019). Synthesis and characterization of ph-sensitive n-succinyl chitosan hydrogel and its properties for biomedical applications. *Journal of the Chilean Chemical Society, 64*(3), 4571–4574. https://doi.org/10.4067/S0717-97072019000304571

Baxter, A., Dillon, M., Anthony Taylor, K. D., & Roberts, G. A. F. F. (1992). Improved method for i.r. determination of the degree of N-acetylation of chitosan. *International Journal of Biological Macromolecules, 14*(3), 166–169. https://doi.org/10.1016/S0141-8130(05)80007-8

Brugnerotto, J., Lizardi, J., Goycoolea, F. M., Argüelles-Monal, W., Desbrières, J., & Rinaudo, M. (2001). An infrared investigation in relation with chitin and chitosan characterization. *Polymer, 42*(8), 3569–3580. https://doi.org/10.1016/S0032-3861(00)00713-8

Cadinoiu, A. N., Rata, D. M., Daraba, O. M., Ichim, D. L., Popescu, I., Solcan, C., & Solcan, G. (2022). Silver nanoparticles biocomposite films with antimicrobial activity: In vitro and in vivo tests. *International Journal of Molecular Science, 23*(18), 10671. https://doi.org/10.3390/ijms231810671

Casadidio, C., Peregrina, D. V., Gigliobianco, M. R., Deng, S., Censi, R., & Di Martino, P. (2019). Chitin and chitosans: Characteristics, eco-friendly processes, and applications in cosmetic science. *Marine Drugs, 17*(6), 369. https://doi.org/10.3390/md17060369

Cele, Z. E. D., Somboro, A. M., Amoako, D. G., Ndlandla, L. F., & Balogun, M. O. (2020). Fluorinated quaternary chitosan derivatives: Synthesis, characterization, antibacterial activity, and killing kinetics. *ACS Omega, 5*(46), 29657–29666. https://doi.org/10.1021/acsomega.0c01355

Chang, S.-H., Lin, H.-T. V., Wu, G.-J., & Tsai, G. J. (2015). pH effects on solubility, zeta potential, and correlation between antibacterial activity and molecular weight of chitosan. *Carbohydrate Polymers, 134*, 74–81. https://doi.org/10.1016/j.carbpol.2015.07.072

Chiloeches, A., Funes, A., Cuervo-Rodríguez, R., López-Fabal, F., Fernández-García, M., Echeverría, C., & Muñoz-Bonilla, A. (2021). Biobased polymers derived from itaconic acid bearing clickable groups with potent antibacterial activity and negligible hemolytic activity. *Polymer Chemistry, 12*(21), 3190–3200. https://doi.org/10.1039/D1PY00098E

CLSI, n.d.CLSI, Methods for Dilution Antimicrobial Susceptibility Tests for Bacteria That Grow Aerobically, Approved Standard-Ninth Edition, CLSI document M07-A9, Clinical and Laboratory Standards Institute, Wayne, PA, 2012. (n.d.).

Cuervo-Rodríguez, R., López-Fabal, F., Gómez-Garcés, J. L., Muñoz-Bonilla, A., & Fernández-García, M. (2017). Contact active antimicrobial coatings prepared by polymer blending. *Macromolecular Bioscience, 17*(11), Article 1700258. https://doi.org/10.1002/mabi.201700258

Dallan, P. R. M., da Luz Moreira, P., Petinari, L., Malmonge, S. M., Beppu, M. M., Genari, S. C., Moraes, A. M., Moreira, P. D. L., Petinari, L., Malmonge, S. M., Beppu, M. M., Genari, S. C., & Moraes, A. M. (2007). Effects of chitosan solution concentration and incorporation of chitin and glycerol on dense chitosan membrane properties. *Journal of Biomedical Materials Research Part B: Applied Biomaterials, 80B*(2), 394–405. https://doi.org/10.1002/jbm.b.30610

Ding, L., Huang, Y., Cai, X., & Wang, S. (2019). Impact of pH, ionic strength and chitosan charge density on chitosan/casein complexation and phase behavior. *Carbohydrate Polymers, 208*, 133–141. https://doi.org/10.1016/j.carbpol.2018.12.015

Guinesi, L. S., & Cavalheiro, É. T. G. (2006). The use of DSC curves to determine the acetylation degree of chitin/chitosan samples. *Thermochimica Acta, 444*(2), 128–133. https://doi.org/10.1016/j.tca.2006.03.003

Harish Prashanth, K. (2002). Solid state structure of chitosan prepared under different N-deacetylating conditions. *Carbohydrate Polymers, 50*(1), 27–33. https://doi.org/10.1016/S0144-8617(01)00371-X

Jayakumar, R., Prabaharan, M., Sudheesh Kumar, P. T., Nair, S. V., & Tamura, H. (2011). Biomaterials based on chitin and chitosan in wound dressing applications. *Biotechnology Advances, 29*(3), 322–337. https://doi.org/10.1016/j.biotechadv.2011.01.005

Jayasuriya, A. C., Aryaei, A., & Jayatissa, A. H. (2013). ZnO nanoparticles induced effects on nanomechanical behavior and cell viability of chitosan films. *Materials Science and Engineering: C, 33*(7), 3688–3696. https://doi.org/10.1016/j.msec.2013.04.057

Jung, J., Wen, J., & Sun, Y. (2019). Amphiphilic quaternary ammonium chitosans self-assemble onto bacterial and fungal biofilms and kill adherent microorganisms. *Colloids and Surfaces B: Biointerfaces, 174*, 1–8. https://doi.org/10.1016/j.colsurfb.2018.10.078

Kasaai, M. R. (2008). A review of several reported procedures to determine the degree of N-acetylation for chitin and chitosan using infrared spectroscopy. *Carbohydrate Polymers, 71*(4), 497–508. https://doi.org/10.1016/j.carbpol.2007.07.009

Kasaai, M. R. (2009). Various methods for determination of the degree of N-acetylation of chitin and chitosan: A review. *Journal of Agricultural and Food Chemistry, 57*(5), 1667–1676. https://doi.org/10.1021/jf803001m

Kaya, M., Khadem, S., Cakmak, Y. S., Mujtaba, M., Ilk, S., Akyuz, L., Salaberria, A. M., Labidi, J., Abdulqadir, A. H., & Deligöz, E. (2018). Antioxidative and antimicrobial edible chitosan films blended with stem, leaf and seed extracts of Pistacia terebinthus for active food packaging. *RSC Advances, 8*(8), 3941–3950. https://doi.org/10.1039/C7RA12070B

Ke, C.-L., Deng, F.-S., Chuang, C.-Y., & Lin, C.-H. (2021). Antimicrobial actions and applications of chitosan. *Polymers, 13*(6), 904. https://doi.org/10.3390/polym13060904

Kumar, S., Mukherjee, A., & Dutta, J. (2020). Chitosan based nanocomposite films and coatings: Emerging antimicrobial food packaging alternatives. *Trends in Food Science & Technology, 97*, 196–209. https://doi.org/10.1016/j.tifs.2020.01.002

Lawrie, G., Keen, I., Drew, B., Chandler-Temple, A., Rintoul, L., Fredericks, P., & Grøndahl, L. (2007). Interactions between alginate and chitosan biopolymers characterized using FTIR and XPS. *Biomacromolecules, 8*(8), 2533–2541. https://doi.org/10.1021/bm070014y

Liang, S., Huang, Q., Liu, L., & Yam, K. L. I. (2009). Microstructure and molecular interaction in glycerol plasticized chitosan/poly(vinyl alcohol) blending films. *Macromolecular Chemistry and Physics, 210*(10), 832–839. https://doi.org/10.1002/macp.200900053

Ma, X., Qiao, C., Wang, X., Yao, J., & Xu, J. (2019). Structural characterization and properties of polyols plasticized chitosan films. *International Journal of Biological Macromolecules, 135*, 240–245. https://doi.org/10.1016/j.ijbiomac.2019.05.158

Maria, V. D., Bernal, C., & Francois, N. J. (2016). Development of biodegradable films based on chitosan/glycerol blends suitable for biomedical applications. *Journal of Tissue Science & Engineering, 07*(03). https://doi.org/10.4172/2157-7552.1000187

Morsy, M., Mostafa, K., Amyn, H., El-Ebissy, A., Salah, A., & Youssef, M. (2019). Synthesis and characterization of freeze dryer chitosan nano particles as multi functional eco-friendly finish for fabricating easy care and antibacterial cotton textiles. *Egyptian Journal of Chemistry, 62*(7), 1277–1293. https://doi.org/10.21608/ejchem.2019.6995.1583

Moussout, H., Ahlafi, H., Aazza, M., & Bourakhouadar, M. (2016). Kinetics and mechanism of the thermal degradation of biopolymers chitin and chitosan using thermogravimetric analysis. *Polymer Degradation and Stability, 130*, 1–9. https://doi.org/10.1016/j.polymdegradstab.2016.05.016

Muñoz-Bonilla, A., Echeverria, C., Sonseca, Á., Arrieta, P. M., & Fernández-García, M. (2019). Bio-based polymers with antimicrobial properties towards sustainable development. *Materials, 12*(4), 641. https://doi.org/10.3390/ma12040641

Nouri, A., Yaraki, M. T., Ghorbanpour, M., Agarwal, S., & Gupta, V. K. (2018). Enhanced antibacterial effect of chitosan film using Montmorillonite/CuO nanocomposite. *International Journal of Biological Macromolecules, 109*, 1219–1231. https://doi.org/10.1016/j.ijbiomac.2017.11.119

Ottey, M. (1996). Compositional heterogeneity of heterogeneously deacetylated chitosans. *Carbohydrate Polymers, 29*(1), 17–24. https://doi.org/10.1016/0144-8617(95)00154-9

Pandit, A. H., Mazumdar, N., Imtiyaz, K., Alam Rizvi, M. M., & Ahmad, S. (2020). Self-healing and injectable hydrogels for anticancer drug delivery: A study with multialdehyde gum arabic and succinic anhydride chitosan. *ACS Applied Bio Materials, 3*(12), 8460–8470. https://doi.org/10.1021/acsabm.0c00835

Pavinatto, A., Mattos, A. V. A., Malpass, A. C. G., Okura, M. H., Balogh, D. T., & Sanfelice, R. C. (2020). Coating with chitosan-based edible films for mechanical/biological protection of strawberries. *International Journal of Biological Macromolecules, 151*, 1004–1011. https://doi.org/10.1016/j.ijbiomac.2019.11.076

Phuangkaew, T., Booranabunyat, N., Kiatkamjornwong, S., Thanyasrisung, P., & Hoven, V. P. (2022). Amphiphilic quaternized chitosan: Synthesis, characterization, and anti-cariogenic biofilm property. *Carbohydrate Polymers, 277*, Article 118882. https://doi.org/10.1016/j.carbpol.2021.118882

Piegat, A., Goszczyńska, A., Idzik, T., & Niemczyk, A. (2019). The importance of reaction conditions on the chemical structure of N,O-acylated chitosan derivatives. *Molecules, 24*(17), 3047. https://doi.org/10.3390/molecules24173047

Pillai, C. K. S. S., Paul, W., & Sharma, C. P. (2009). Chitin and chitosan polymers: Chemistry, solubility and fiber formation. *Progress in Polymer Science, 34*(7), 641–678. https://doi.org/10.1016/j.progpolymsci.2009.04.001

Policastro, D., Giorno, E., Scarpelli, F., Godbert, N., Ricciardi, L., Crispini, A., Candreva, A., Marchetti, F., Xhafa, S., De Rose, R., Nucera, A., Barberi, R. C., Castriota, M., De Bartolo, L., & Aiello, I. (2022). New zinc-based active chitosan films: Physicochemical characterization, antioxidant, and antimicrobial properties. *Frontiers in Chemistry, 10*, Article 884059. https://doi.org/10.3389/fchem.2022.884059

Pranantyo, D., Xu, L. Q., Kang, E.-T. T., & Chan-Park, M. B. (2018). Chitosan-based peptidopolysaccharides as cationic antimicrobial agents and antibacterial coatings. *Biomacromolecules, 19*(6), 2156–2165. https://doi.org/10.1021/acs.biomac.8b00270

Sabbah, M., Di Pierro, P., Cammarota, M., Dell'Olmo, E., Arciello, A., & Porta, R. (2019). Development and properties of new chitosan-based films plasticized with spermidine and/or glycerol. *Food Hydrocolloids, 87*, 245–252. https://doi.org/10.1016/j.foodhyd.2018.08.008

Sahariah, P., & Másson, M. (2017). Antimicrobial chitosan and chitosan derivatives: A review of the structure-activity relationship. *Biomacromolecules, 18*(11), 3846–3868. https://doi.org/10.1021/acs.biomac.7b01058

Shagdarova, B., Lunkov, A., Il'ina, A., & Varlamov, V. (2019). Investigation of the properties of N-[(2-hydroxy-3-trimethylammonium) propyl] chloride chitosan derivatives. *International Journal of Biological Macromolecules, 124*, 994–1001. https://doi.org/10.1016/j.ijbiomac.2018.11.209

Si, Z., Hou, Z., Vikhe, Y. S., Thappeta, K. R. V., Marimuthu, K., De, P. P., Ng, O. T., Li, P., Zhu, Y., Pethe, K., & Chan-Park, M. B. (2021). Antimicrobial effect of a novel chitosan derivative and its synergistic effect with antibiotics. *ACS Applied Materials & Interfaces, 13*(2), 3237–3245. https://doi.org/10.1021/acsami.0c20881

Song, X., Liu, L., Wu, X., Liu, Y., & Yuan, J. (2021). Chitosan-based functional films integrated with magnolol: Characterization, antioxidant and antimicrobial activity and pork preservation. *International Journal of Molecular Sciences, 22*(15), 7769. https://doi.org/10.3390/ijms22157769

Song, X., Wang, L., Liu, L., Li, J., & Wu, X. (2022). Impact of tea tree essential oil and citric acid/choline chloride on physical, structural and antibacterial properties of chitosan-based films. *Food Control, 141*, Article 109186. https://doi.org/10.1016/j.foodcont.2022.109186

Taboada, E., Cabrera, G., & Cardenas, G. (2004). Synthesis and characterization of new arylamine chitosan derivatives. *Journal of Applied Polymer Science, 91*(2), 807–812. https://doi.org/10.1002/app.13171

Tejero, R., López, D., López-Fabal, F., Gómez-Garcés, J. L., & Fernández-García, M. (2015). Antimicrobial polymethacrylates based on quaternized 1,3-thiazole and 1,2,3-triazole side-chain groups. *Polymer Chemistry, 6*(18), 3449–3459. https://doi.org/10.1039/C5PY00288E

Van de velde, K., & Kiekens, P. (2004). Structure analysis and degree of substitution of chitin, chitosan and dibutyrylchitin by FT-IR spectroscopy and solid state C NMR. *Carbohydrate Polymers, 58*(4), 409–416. https://doi.org/10.1016/j.carbpol.2004.08.004

Wang, X., Yong, H., Gao, L., Li, L., Jin, M., & Liu, J. (2019). Preparation and characterization of antioxidant and pH-sensitive films based on chitosan and black soybean seed coat extract. *Food Hydrocolloids, 89*, 56–66. https://doi.org/10.1016/j.foodhyd.2018.10.019

Wanjun, T., Cunxin, W., & Donghua, C. (2005). Kinetic studies on the pyrolysis of chitin and chitosan. *Polymer Degradation and Stability, 87*(3), 389–394. https://doi.org/10.1016/j.polymdegradstab.2004.08.006

Wu, M., Long, Z., Xiao, H., & Dong, C. (2016). Recent research progress on preparation and application of N, N, N-trimethyl chitosan. *Carbohydrate Research, 434*, 27–32. https://doi.org/10.1016/j.carres.2016.08.002

Yeh, J.-T., Chen, C.-L., Huang, K. S., Nien, Y. H., Chen, J. L., & Huang, P. Z. (2006). Synthesis, characterization, and application of PVP/chitosan blended polymers. *Journal of Applied Polymer Science, 101*(2), 885–891. https://doi.org/10.1002/app.23517

Zakaria, Z., Izzah, Z., Jawaid, M., & Hassan, A. (2012). Chitosan deacetylation. In , *Vol. 7, Issue 4. BioResources*.

Zhang, J., Tan, W., Luan, F., Yin, X., Dong, F., Li, Q., & Guo, Z. (2018). Synthesis of quaternary ammonium salts of chitosan bearing halogenated acetate for antifungal and antibacterial activities. *Polymers, 10*(5), 530. https://doi.org/10.3390/polym10050530

Zhang, L., Chen, D., Yu, D., Regenstein, J. M., Jiang, Q., Dong, J., Chen, W., & Xia, W. (2022). Modulating physicochemical, antimicrobia and release properties of chitosan/zein bilayer films with curcumin/nisin-loaded pectin nanoparticles. *Food Hydrocolloids, 133*, Article 107955. https://doi.org/10.1016/j.foodhyd.2022.107955

Zhang, X., Ismail, B. B., Cheng, H., Jin, T. Z., Qian, M., Arabi, S. A., Liu, D., & Guo, M. (2021). Emerging chitosan-essential oil films and coatings for food preservation - A review of advances and applications. *Carbohydrate Polymers, 273*, Article 118616. https://doi.org/10.1016/j.carbpol.2021.118616

Ziani, K., Oses, J., Coma, V., & Maté, J. I. (2008). Effect of the presence of glycerol and Tween 20 on the chemical and physical properties of films based on chitosan with different degree of deacetylation. *LWT - Food Science and Technology, 41*(10), 2159–2165. https://doi.org/10.1016/j.lwt.2007.11.023